



# Separation of non-stationary sound fields using single layer pressure-velocity measurements

Chuan-Xing BI<sup>1</sup>; Lin GENG<sup>2</sup>; Xiao-Zheng ZHANG<sup>3</sup>

<sup>1,2,3</sup> Hefei University of Technology, People's Republic of China

## ABSTRACT

This paper presents a sound field separation technique using single layer pressure-velocity measurements to extract the non-stationary signal generated by a target source in the presence of disturbing sources. In the technique, the time-independent pressure and particle velocity signals on one measurement plane are first measured; then the pressure signal generated by the target source alone can be extracted by a simple superposition of the measured pressure and the convolution between the measured particle velocity and the corresponding impulse response function. An experiment involving three speakers driven by a non-stationary signal was investigated, where a pressure-velocity probe was used repeatedly to measure the time-independent pressure and particle velocity signals on the measurement surface and a trigger was used to keep the measured signals the same at each measurement. The experimental results demonstrate that the proposed technique is effective in extracting the desired non-stationary sound field generated by the target source alone from the mixed one both in time and space domains.

Keywords: Non-stationary sound field, Sound field separation, Pressure-velocity measurements  
I-INCE Classification of Subjects Number(s): 75.7

## 1. INTRODUCTION

The field separation method (FSM) has been successfully applied in a complex noisy environment to separate the desired sound field generated by a target source and suppress the influence of disturbing sources. Several different FSMs (1-7) have been presented for regular- or irregular-shaped sources. The separation process in these FSMs can be performed with either double layer pressure-pressure (1-3) or velocity-velocity (4) measurements or single layer pressure-velocity measurements (5-7). However, these FSMs are all performed in the frequency domain. Since non-stationary source whose statistical properties fluctuate in time is often encountered in practical engineering, it is more reasonable to study the non-stationary field separation technique for extracting the acoustic characteristics of a target source in both spatial and time domains.

On the basis of the time-independent pressure-pressure data measured on two closely spaced parallel surfaces and the impulse response function relating pressure to pressure, Zhang *et al.* (8) developed a technique to separate the non-stationary signals generated by a target source in both time and spatial domains. In that technique, the separation accuracy is depended on the distance between the two measurement surfaces and the stabilization of solving the deconvolution process. Recently, a real-time field separation method (RT-FSM) with pressure and particle acceleration measurements on single surface is presented by Bi *et al.* (9), where the particle acceleration is approximately obtained by the finite difference approximation with the pressures measured on two surfaces. In this paper, an alternative method, namely field separation method based on single layer pressure-velocity measurements, is proposed to separate the non-stationary sound field. The difference between the proposed method and the RT-FSM is that the time-independent particle velocity is directly measured by a Microflown pressure-velocity (p-u) probe.

---

<sup>1</sup> cxbi@hfut.edu.cn

<sup>2</sup> genglin20070553@126.com

<sup>3</sup> xzhengzhang@hotmail.com

## 2. THEORETICAL BACKGROUND

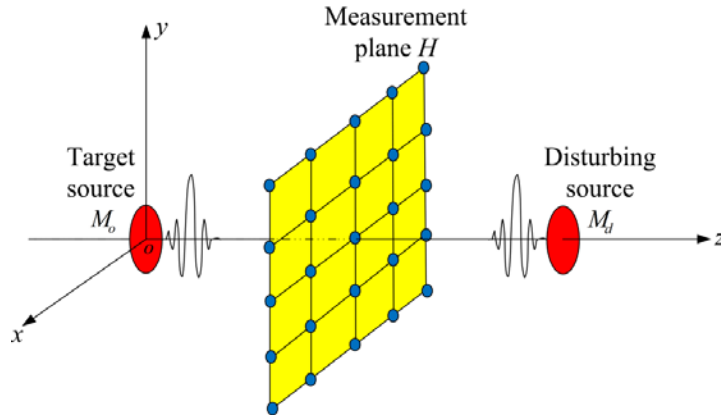


Figure 1 – Geometry of the proposed method in the Cartesian coordinate system  $o(x, y, z)$

Figure 1 illustrates the geometry of the proposed method in the Cartesian coordinate system  $o(x, y, z)$ . The purpose of the present paper is to remove the influence of the disturbing source  $M_d$  and extract the time-evolving pressure signal generated by the target source  $M_o$  from the mixed one. According to the superposition principle of waves, the mixed pressure signal  $p(x, y, z_H, t)$  and the mixed particle velocity signal  $v(x, y, z_H, t)$  at the measurement point  $(x, y, z_H)$  at the time  $t$  can be expressed, respectively, as

$$p(x, y, z_H, t) = p_o(x, y, z_H, t) + p_d(x, y, z_H, t) \quad (1)$$

$$v(x, y, z_H, t) = v_o(x, y, z_H, t) - v_d(x, y, z_H, t) \quad (2)$$

where the subscripts “o” and “d” denote the fields generated by the target source and the disturbing source, respectively.

By applying a two-dimensional Fourier transform with respect to  $x$  and  $y$  to Eqs. (1) and (2), it yields

$$P(k_x, k_y, z_H, t) = P_o(k_x, k_y, z_H, t) + P_d(k_x, k_y, z_H, t) \quad (3)$$

$$V(k_x, k_y, z_H, t) = V_o(k_x, k_y, z_H, t) - V_d(k_x, k_y, z_H, t) \quad (4)$$

where  $k_x$  and  $k_y$  represent the wavenumber components in  $x$  and  $y$  directions, respectively.

The time-wavenumber spectrum of the pressure and particle velocity produced by the same source at the time  $t$  can be expressed, respectively, as

$$P_o(k_x, k_y, z_H, t) = V_o(k_x, k_y, z_H, t) * h(k_x, k_y, 0, t) \quad (5)$$

$$P_d(k_x, k_y, z_H, t) = V_d(k_x, k_y, z_H, t) * h(k_x, k_y, 0, t) \quad (6)$$

where the asterisk denotes the convolution of two time functions. The impulse response function  $h(k_x, k_y, 0, t)$  is given by (10)

$$h(k_x, k_y, 0, t) = \rho_0 c \delta(t) - \rho_0 c^2 \sqrt{k_x^2 + k_y^2} J_1 \left( \sqrt{c^2 (k_x^2 + k_y^2)} t \right) H(t) \quad (7)$$

where  $\rho_0$  is the medium density,  $c$  is the sound velocity,  $\delta(t)$  is the Dirac function,  $J_1$  is the Bessel function of the first kind of order one, and  $H(t)$  is the Heaviside function.

By combining Eqs. (3) and (4) with Eqs. (5) and (6), the time-wavenumber spectrum of the pressure  $P_o(k_x, k_y, z_H, t)$  can be finally obtained by

$$P_o(k_x, k_y, z_H, t) = 0.5 [P(k_x, k_y, z_H, t) + V(k_x, k_y, z_H, t) * h(k_x, k_y, 0, t)] \quad (8)$$

To meet the requirement of numerical computation, the time  $t$  is discretized by

$$t_n = (n-1)\Delta t \quad (9)$$

where  $n = 1, 2, \dots, N$ ,  $N$  is the total number of time steps, and  $\Delta t$  is the time step. Accordingly, Eq. (8) can be expressed in a discrete form as follows

$$P_o(k_x, k_y, z_H, t_n) = 0.5[P(k_x, k_y, z_H, t_n) + \sum_{i=1}^n V(k_x, k_y, z_H, t_i)h(k_x, k_y, 0, t_{n-i+1})] \quad (10)$$

From Eq. (10), it is noted that once the mixed pressure spectrum at the time instant  $t_n$  and the mixed particle velocity spectrums from the time instant  $t_1$  to the time instant  $t_n$  are known, the pressure spectrum  $P_o(k_x, k_y, z_H, t_n)$  at the time instant  $t_n$  can be extracted. Then, the two-dimensional inverse Fourier transform with respect to  $k_x$  and  $k_y$  is applied to the pressure spectrum  $P_o(k_x, k_y, z_H, t_n)$  to obtain the pressure  $p_o(x, y, z_H, t_n)$ .

### 3. EXPERIMENT

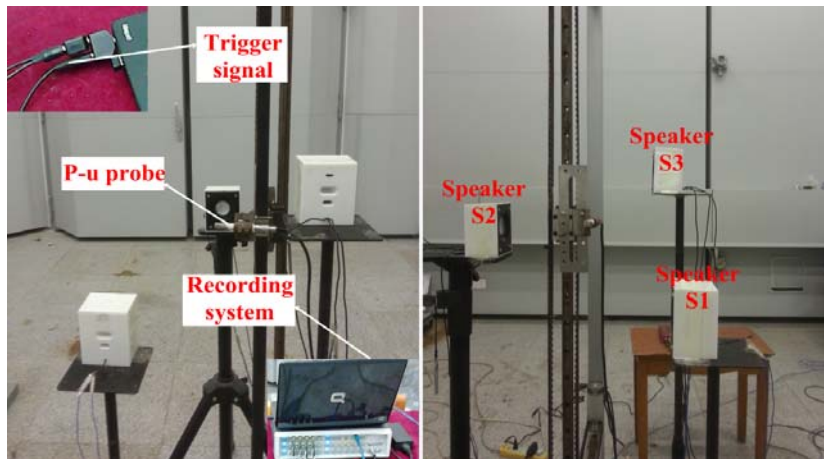


Figure 2 – Experimental setup

An experiment has been carried out in a semi-anechoic chamber to demonstrate the feasibility of the proposed method. The experimental setup was depicted in Figure 2. Three speakers S1, S2 and S3 were used as the sources to generate a non-stationary mixed sound field. The speakers S1 and S3 were the target sources, and the speakers S2 was the disturbing source. All speakers were driven by the same signal defined by

$$s(t) = 0.6 \cos(2\pi f_0 t) e^{-10^6 (t-0.005)^2 / 2} \quad (11)$$

where  $f_0=344$  Hz. A p-u probe was repeatedly used to measure the time-independent pressure and particle velocity signals at  $9 \times 9$  measurement points. To keep the measured signals the same at each measurement, the output of the source signal was set as the trigger to activate the acquisition system recording the data. It should be noted that the amplitude and phase sensitivities of pressure and of particle velocity in the frequency domain can be found in the calibration report of the probe provided by the manufacturer. The time domain calibration factors of pressure and particle velocity can be obtained by applying the inverse Fourier transform to the corresponding frequency domain calibration factors. The calibrated time-independent pressure and particle velocity can be obtained by the convolution of the recorded signal and the corresponding time domain calibration factor.

As shown in Figure 3, the measurement plane  $H$  was positioned on the plane  $z=0$ .  $9 \times 9$  measurement points were distributed on the plane  $H$ , and the grid space was 0.06 m in both  $x$  and  $y$  directions. The centers of the speakers S1, S2 and S3 were located at (0.12 m, 0.12 m, -0.15 m), (0.24 m, 0.24 m, 0.16 m) and (0.42 m, 0.3 m, -0.14 m), respectively. The signals were sampled at a frequency of  $f_e=25.6$  kHz, providing 1024 sampling points.

The time-domain pressure waveform comparisons at three space points  $R_1(0.12$  m, 0.12 m, 0 m),  $R_2(0.24$  m, 0.24 m, 0 m), and  $R_3(0.42$  m, 0.3 m, 0 m) on the plane  $H$  are depicted in Figure 4, in which the solid line, the line with plus sign and the dotted line denote the measured pressure radiated by the target sources, the mixed pressure including the contributions of all sources and the extracted pressure by using the proposed method, respectively. It can be seen from the comparisons of the solid lines and the lines with plus sign at these points that time-domain pressure waveforms of target sources have

been changed by the disturbing source  $S2$  in different degrees. The comparison results between the solid lines and the dotted lines shown in Figure 4 indicate that the changes in both the phase and amplitude can be corrected by the proposed method and the extracted pressures match well with the measured pressures.

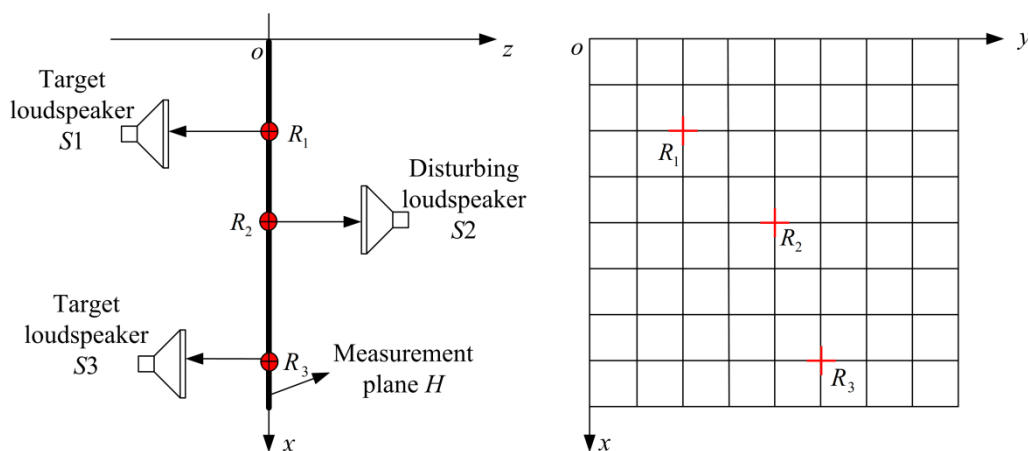


Figure 3 – Geometry of the measurement plane  $H$  and the locations of three speakers. Three space points  $R1$ ,  $R2$ , and  $R3$  are chosen and marked with the symbol “+”. The points  $R1$  and  $R3$  were facing the target sources  $S1$  and  $S3$ , respectively, and the point  $R2$  was facing the disturbing source  $S2$

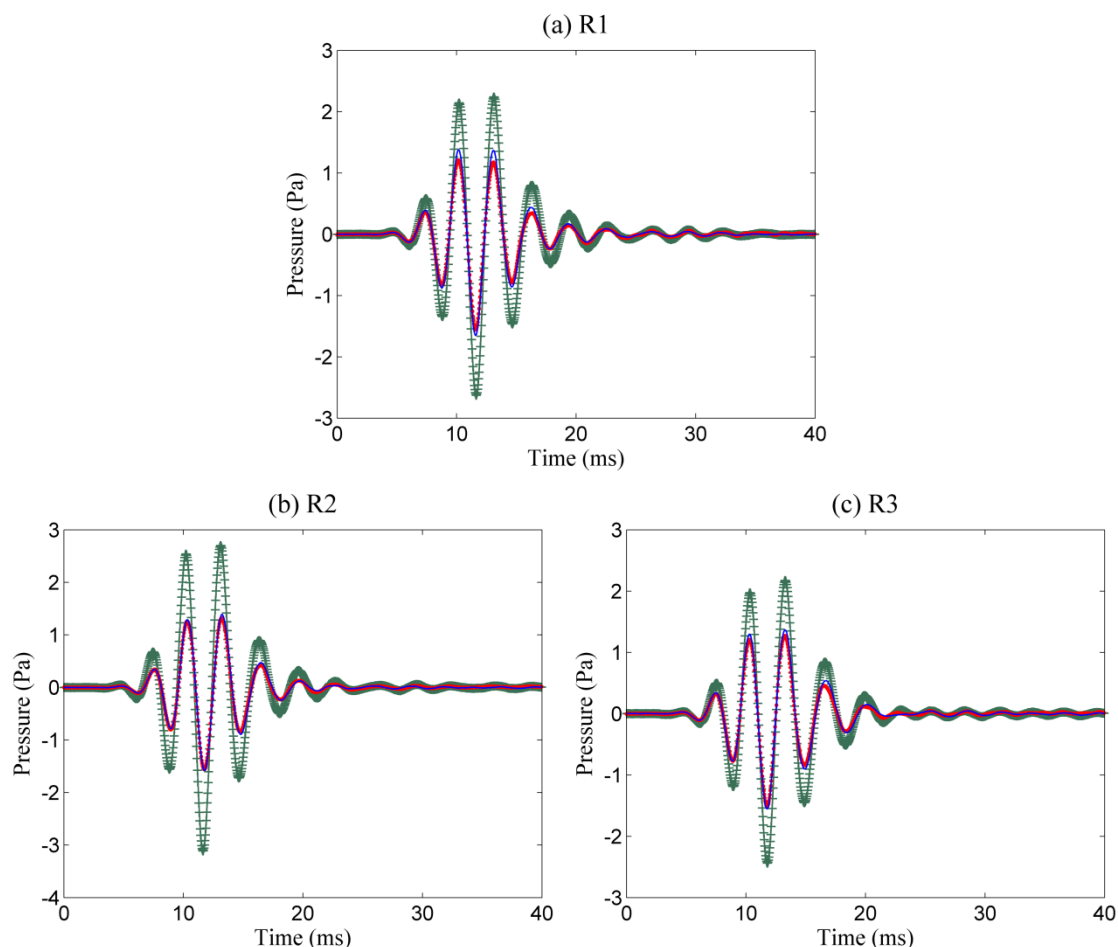


Figure 4 – Time-domain waveform comparisons among the measured pressure radiated by the target sources (solid line), the mixed pressure including contributions of all sources (line with plus sign), and the extracted pressure by using the proposed method (dotted line) at three space points (a)  $R1$ , (b)  $R2$ , and (c)  $R3$

For a quantitative comparison, two indicators  $T_1$  and  $T_2$  are defined to assess the phase similarity and the amplitude difference (the definitions of  $T_1$  and  $T_2$  can be found in reference (11)). The phase accuracy gives  $T_1$  in the neighborhood of 1, and the amplitude accuracy gives  $T_2$  near 0.

In order to quantify the accuracy of the proposed method on the whole measurement plane  $H$ , the phase indicator  $T_1$  and the amplitude indicator  $T_2$  of the time-domain pressure waveforms are calculated at each space point and the maps are shown in Figure 5. The values of  $T_1$  and  $T_2$  at a majority of space points are more than 0.96 and below 0.1, respectively, which indicates that the extracted time-evolving pressure signals and the measured ones achieve the high phase similarity and little amplitude difference at all space points. Here, the calculated values of  $T_1$  at the selected three points  $R_1$ ,  $R_2$ , and  $R_3$  are 0.9987, 0.9982 and 0.9983, respectively, and the values of  $T_2$  are 0.1006, 0.0289 and 0.0683, respectively.

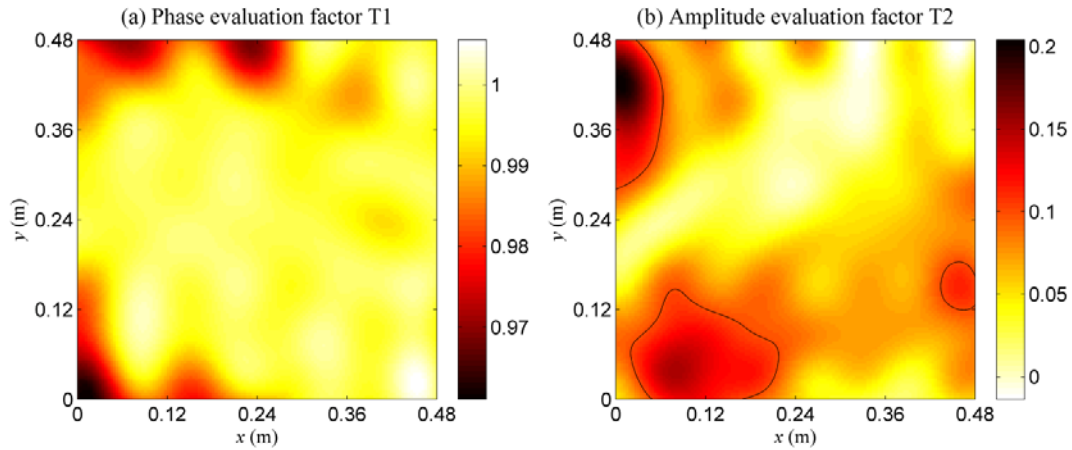


Figure 5 – Spatial maps of (a) phase indicator  $T_1$  and (b) amplitude indicator  $T_2$  with a contour line at the value of 0.1.

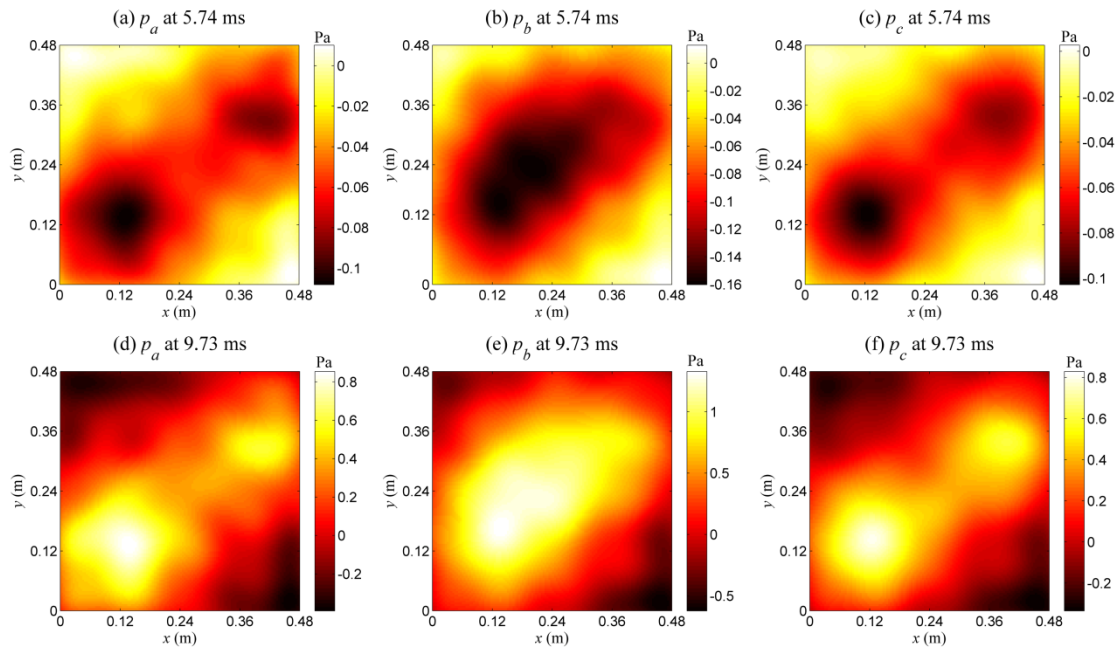


Figure 6 – Spatial distributions of the measured pressure fields  $p_a$  at (a)  $t_1=5.74$  ms and (d)  $t_2=9.73$  ms, the mixed pressure fields  $p_b$  at (b)  $t_1=5.74$  ms and (e)  $t_2=9.73$  ms, and the extracted pressure fields  $p_c$  at (c)  $t_1=5.74$  ms and (f)  $t_2=9.73$  ms on the measurement plane  $H$ .

Since the time-domain pressure waveforms at all the space points are contaminated by the disturbing source  $S_3$ , the spatial distribution of the measured pressure field  $p_a$  at any time instant would also be changed. Just as the comparison of time-domain waveforms, two time instants  $t_1=5.74$

ms and  $t_2=9.73$  ms are selected to display the extracted results in the space domain. The measured pressure field  $p_a$ , the mixed pressure field  $p_b$ , and the extracted pressure field  $p_c$  at  $t_1=5.74$  ms are depicted in Figures 6(a), 6(b), and 6(c), respectively. Figures 6(d), 6(e), and 6(f) depict the same pressure fields but at  $t_2=9.73$  ms. It is observed that the mixed pressure fields  $p_b$  in Figures 6(b) and 6(e) are very different from the pressure fields  $p_a$  in Figures 6(a) and 6(d), which indicates that the contamination should be removed before studying the transient sound radiation of the target sources alone. After using the proposed method, the distributions of the extracted pressure fields  $p_c$  in Figures 6(c) and 6(f) are in good accordance with the measured ones in Figures 6(a) and 6(b) at these two time instants, which evidences that the proposed method presented in this paper is effective in extracting the pressure field generated by the target sources alone at any time instant when the disturbing source S3 exists synchronously.

#### 4. CONCLUSIONS

With the aid of single layer pressure-velocity measurements, an extraction method is developed to separate the non-stationary sound field radiated by a target source from the mixed one when the disturbing sources exist on the other side of the measurement plane. In the method, the pressure and particle velocity on the measurement plane are measured by a Microflown p-u probe. The pressure signal from the target source alone can be extracted by combining the measured pressure-velocity data and the corresponding impulse response function. An experiment with two speakers as the target sources and one as the disturbing source was carried out to validate the proposed method. The experimental results demonstrated that the proposed method could correct the changes in the time-evolving pressure belonging to target sources very well. The separation results indicated the satisfactory agreements both for the time-evolving pressure signal at a specific space point and for the pressure field mode shape at a specific time instant.

#### ACKNOWLEDGEMENTS

This work was supported by the National Natural Science Foundation of China (Grant Nos. 51322505 and 11274087).

#### REFERENCES

1. Tamura M. Spatial Fourier transform method of measuring reflection coefficients at oblique incidence. I: Theory and numerical examples. *J Acoust Soc Am.* 2009; 88(5):2259-2264.
2. Zhao X, Wu SF. Reconstruction of vibroacoustic fields in half-space by using hybrid near-field acoustical holography. *J Acoust Soc Am.* 2005; 117(2): 555-565.
3. Bi CX, Chen XZ, Chen J. Sound field separation technique based on equivalent source method and its application in nearfield acoustic holography. *J Acoust Soc Am.* 2008; 123(3): 1472-1478.
4. Fernandez-Grande E, Jacobsen F. Sound field separation with a double layer velocity transducer array (L). *J Acoust Soc Am.* 2011; 130(1): 5-8.
5. Jacobsen F, Jaud V. Statistically optimized near field acoustic holography using an array of pressure-velocity probes. *J Acoust Soc Am.* 2007; 121(3): 1550-1558.
6. Fernandez-Grande E, Jacobsen F, Leclère Q. Sound field separation with sound pressure and particle velocity measurements. *J Acoust Soc Am.* 2012; 132(6): 3818-3825.
7. Braikia Y, Melon M, Langrenne C, Bavu É, Garcia A. Evaluation of a separation method for source identification in small spaces. *J Acoust Soc Am.* 2013; 134(1): 323-331.
8. Zhang XZ, Thomas JH, Bi CX, Pascal JC. Separation of non-stationary sound fields in the time-wavenumber domain. *J Acoust Soc Am.* 2012; 131(3): 2180-2189.
9. Bi CX, Geng L, Zhang XZ. Real-time separation of nonstationary sound fields with pressure and particle acceleration measurements. *J Acoust Soc Am.* 2014; 135(6): 3474- 3482.
10. Zhang XZ, Bi CX, Zhang YB, Geng L. Real-time nearfield acoustic holography for reconstructing the instantaneous surface normal velocity. *Mech Syst Signal Process.* 2014; <http://dx.doi.org/10.1016/j.ymsp.2014.06.009>
11. Paillasseur S, Thomas JH, Pascal JC. Regularization for improving the deconvolution in real-time near-field acoustic holography. *J Acoust Soc Am.* 2011; 129(6): 3777-3787.